ISBN: 978-3-95450-231-8 ISSN: 2673-5490 doi: 10.18429/JACoW-IPAC2023-TUPL039

# BAYESIAN OPTIMIZATION FOR HIGH-POWER X-RAY VORTEX GENERATION

J. W. Yan*, G. Geloni, European XFEL, Schenefeld, Germany

*Abstract*

X-ray beams with orbital angular momentum (OAM) have emerged as a powerful tool for investigating matter. Traditional optical elements, such as spiral phase plates and zone plates, have been employed to generate OAM light. However, applying these elements in x-ray free-electron lasers (XFELs) remains challenging due to high impinging intensities and efficiency concerns. The self-seeded FEL with OAM (SSOAM) method has been recently proposed to generate intense x-ray vortices, overcoming these limitations. In this study, we focus on optimizing the SSOAM scheme to enhance the production of high-power x-ray vortices. A Bayesian optimization approach is employed to optimize the undulator tapering, ensuring the efficient generation of x-ray OAM pulses in XFELs.

## INTRODUCTION

Structured light generation can offer new insights into various physical phenomena. Optical vortices, carrying orbital angular momentum (OAM) and characterized by a helical phase-front, have been extensively studied and utilized in fields such as optical tweezers, quantum entanglement, super-resolution microscopy, and optical data transmission [1, 2]. Short-wavelength OAM beams, in particular, can initiate new phenomena through light-matter interactions and hold potential for applications in areas such as quadrupolar x-ray dichroism, photoionization, resonant inelastic x-ray scattering, and time-resolved twisted x-ray diffraction [3–6].

Modern x-ray free-electron lasers (FELs) deliver high-brightness pulses ranging from tens of femtoseconds to attoseconds, enabling research across multiple scientific disciplines [7]. Most x-ray FEL facilities worldwide employ the self-amplified spontaneous emission (SASE) mechanism, which operates over a wide spectral range, reaching sub-angstrom wavelengths. Self-seeding schemes have been suggested to enhance the temporal coherence and spectral density of FEL pulses [8]. However, the transverse FEL radiation profile of both SASE and self-seeding schemes at saturation is typically Gaussian-like [9].

A straightforward method for generating x-ray OAM light involves using optical elements, such as spiral phase plates (SPP) [10, 11], spiral Fresnel zone plates (SZP) [12, 13], and diffractive optics [14], placed after the undulator. These elements, well-developed and experimentally demonstrated to produce soft and hard x-ray OAM light at synchrotron sources, face challenges regarding thermal loading and efficiency when applied to XFELs with high pulse energies. These challenges become even more critical in high-repetition-rate XFELs based on superconducting accelerators.

Various XFEL operation modes have been proposed to generate OAM light, including using helical undulators [15, 16], forming electron bunches with helical shapes [17,18], or XFEL oscillators [19]. Nonetheless, these methods exhibit limitations, such as weaker harmonic emissions, seed laser availability, and harmonic conversion numbers. Generating OAM light with the XFEL oscillator requires a substantial upgrade of the modern XFEL facilities. Consequently, there is significant interest in creating intense OAM light in planar undulators using the widely adopted SASE or self-seeding operation modes.

Recently, a self-seeded FEL with OAM (SSOAM) method [20] has been proposed to generate high-power x-ray vortices. This approach does not require helical undulators or external seed laser systems, making it suitable for all existing XFEL user facilities with minimal hardware addition, especially when integrated with self-seeding setups. In this paper, we introduce the Bayesian optimization method for efficiently optimizing the SSOAM scheme.

## PRINCIPLE OF THE SSOAM SCHEME

The schematic layout of the SSOAM scheme is depicted in Fig. 1. In this scheme, the undulator is divided into two stages. The first stage operates in SASE mode to generate a relatively weak seed pulse. An optical element, such as an SPP or SZP, is then used to imprint the helical phase of a low-order OAM mode onto the FEL beam, creating an OAM seed pulse. A small magnetic chicane, situated between the first and second stages, is necessary to divert the electron bunch and eliminate the microbunching introduced in the first stage, resulting in a minor delay of fewer than ten femtoseconds between the OAM seed and the electron bunch. Finally, the OAM seed pulse interacts with the electron beam in the second-stage undulator and is substantially amplified. In this scheme, a relatively long electron bunch or fresh-slice operation is required to ensure the amplification of the OAM seed in the second stage.

As emphasized in [20], the seed pulse generated in the first stage is not a pure Gaussian pulse, suggesting that multiple transverse mode competition will occur in the second-stage undulator. Assuming a helical phase of $\exp(i\phi)$ is introduced by an SPP, the $l = 0$ mode in the first stage will be transformed to the $l = 1$ mode in the second stage and amplified. Consequently, in the SSOAM scheme, it is crucial to optimize the first-stage undulator to ensure high mode purity of the $l = 0$ mode and the second-stage undulator to guarantee effective amplification of the $l = 1$ mode.

* jiawei.yan@xfel.eu

ISBN: 978-3-95450-231-8 ISSN: 2673-5490 doi: 10.18429/JACoW-IPAC2023-TUPL039



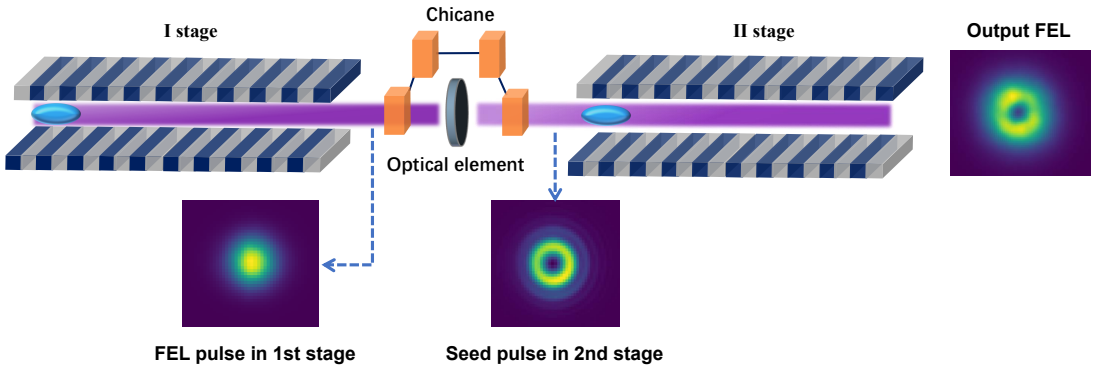


Figure 1: Schematic layout of the SSOAM scheme.

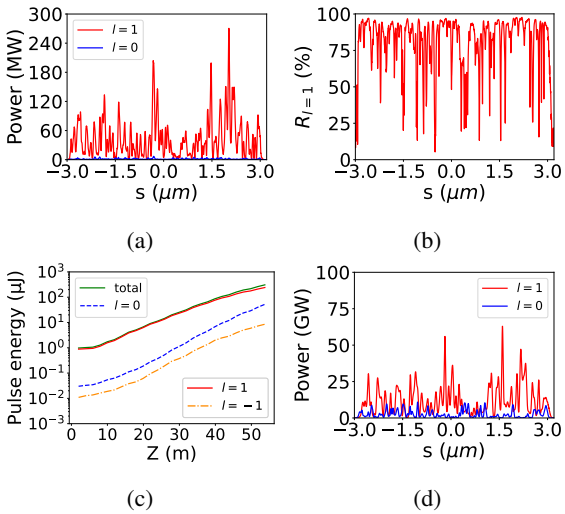


Figure 2: (a) Temporal power of the FEL seed pulse at the entrance of the second-stage undulator. (b) Ratio of the $l = 1$ mode along the FEL seed pulse. (c) Gain curves of different OAM modes along the second stage. (d) Temporal power of the FEL pulse at the end of the second-stage undulator.

In this work, we adopt the same simulation framework as detailed in [20]. We consider a 14 GeV electron beam characterized by a normalized emittance of 0.5 mm.mrad, a bunch length of 20 femtoseconds, and a flat-top current profile of 5000 A. These parameters have been selected to produce FEL pulses at 9 keV. For the first-stage undulator, the configuration follows the original SSOAM paper [20], utilizing nine undulator cells with a slight reverse taper. The FEL pulse generated in the initial stage then passes through an SPP, where a helical phase of $\exp(i\phi)$ is introduced, and an efficiency of 10% is assumed. The power profile of the OAM seed pulse at the entrance of the second-stage undulator is illustrated in Fig. 2(a). The pulse energy of the OAM seed pulse is approximately 0.96 μJ. The mode decomposition of the pulse reveals that the relative weights of the $l = 0$, $l = -1$, and $l = 1$ modes are 91%, 3%, and 3%, respectively. The ratio of the $l = 1$ mode along the seed pulse is depicted in Fig. 2(b). In the original SSOAM paper [20], a linear taper is adopted for the second-stage undulator, and a fresh electron bunch is employed to amplify the OAM seed pulse. The gain curve of the FEL pulse along the second-stage undulator is presented in Fig. 2(c), where nine undulator cells are utilized. As demonstrated in Fig. 2(d), at the end of the undulator, the FEL pulse is amplified to 307.94 μJ. The ratio of the $l = 1$ mode in the amplified pulse is around 78%. The $l = 0$ mode is also amplified in portions of the electron beam with relatively weak OAM seed power, which is the primary cause of the mode purity drop for the entire pulse. However, for those parts with strong OAM seed power, the power and purity of the $l = 1$ mode remain high. One possible approach to further improve the scheme is by optimizing the taper configuration of the second-stage undulator to favor the amplification of the $l = 1$ mode.

## BAYESIAN OPTIMIZATION OF THE UNDULATOR TAPERING

Undulator tapering is a critical technique for obtaining high-power FEL pulses, particularly in self-seeding operations. Taper optimization has garnered significant interest over the past decades, and various strategies have been proposed to address this optimization challenge [21]. Intelligent algorithms, such as multi-objective evolutionary algorithms (MOEAs), offer an effective means for optimizing undulator tapering [22]. However, MOEAs typically require a large number of objective evaluations, which can be time-consuming for both simulation-based optimization and online experiments.

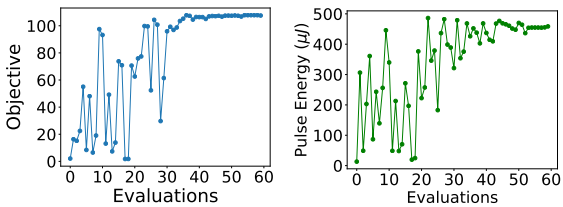


Figure 3: Objective values (a) and pulse energy of the FEL pulse (b) at different evaluations.

ISBN: 978-3-95450-231-8 ISSN: 2673-5490 doi: 10.18429/JACoW-IPAC2023-TUPL039

Bayesian optimization [23, 24] is a probabilistic model-based algorithm that utilizes prior knowledge and uncertainty to guide the optimization process. By incorporating Gaussian processes [25], Bayesian optimization can capture uncertainty and efficiently explore the search space, resulting in a balance between exploration and exploitation. In recent years, Bayesian optimization has gained considerable attention due to its potential for hyperparameter tuning in neural networks [26]. More recently, Bayesian optimization has been proposed for efficient online control of particle accelerators and XFELs [27, 28]. In this study, we employ Bayesian optimization to efficiently optimize undulator tapering within the SSOAM scheme.

We perform piecewise optimization of the second-stage undulator. The field strength of the initial undulator cell, the linear taper term, and the quadratic taper term are optimized using Bayesian optimization. In the SSOAM scheme, our goal is to obtain an XFEL pulse with both high peak power and good purity of the OAM mode simultaneously. As such, we set the optimization objective as $P^{R_{l=1}}$, where P represents the pulse energy, and $R_{l=1}$ denotes the ratio of the $l = 1$ mode in the entire pulse.

During the optimization process, Gaussian process regression is employed to construct a probabilistic model for the objective, with 20 random samples utilized to initialize the Gaussian process model. The upper confidence bound [29] serves as the acquisition function. Fig.3 displays the results of the Bayesian optimization. After 60 evaluations, the objective value converges to approximately 108. Fig.4 depicts a typical optimized case, in which the pulse energy reaches 458.67 µJ, and the ratio of the $l = 1$ mode is 76%. Overall, the $l = 1$ mode has been amplified around 400 times in the second stage. Compared to the results presented in Fig. 2, the pulse energy has increased by 48.95%. Fig.4(a) illustrates the power profile of the FEL pulse at the end of the second-stage undulator. Fig.4(b) shows the ratio of the $l = 1$ mode along the pulse, indicating that the high-power portion of the FEL pulse maintains good mode purity. Fig.4(c) and Fig.4(d) present the transverse profile and transverse phase distribution at the peak power position of the FEL pulse, respectively.

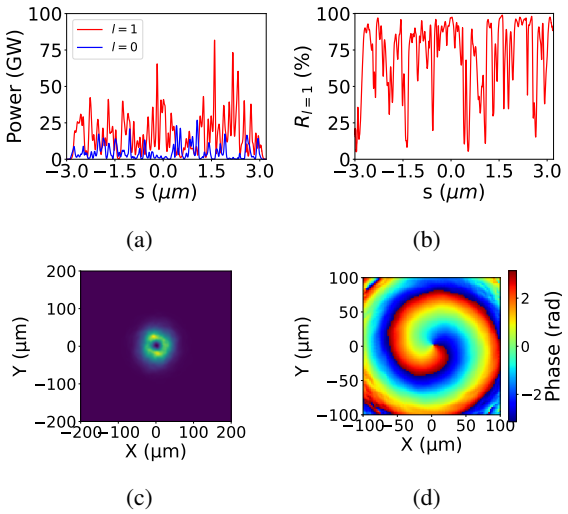


Figure 4: Temporal power (a) and ratio of the $l = 1$ mode (b) of the FEL pulse at the end of the second-stage undulator, obtained using the optimized undulator tapering. Transverse profile (c) and transverse phase distribution (d) at the position of maximum power in the pulse.

## CONCLUSION

In summary, this study demonstrates the application of Bayesian optimization for undulator tapering in the SSOAM scheme, aiming to enhance the x-ray OAM pulse generation. The optimization results reveal that the SSOAM scheme holds promise as a method for generating intense x-ray OAM pulses. It is important to note that the optimization presented here is merely a first step. More systematic optimization efforts, including undulator tapering for both the first and second stages, electron beam size, and quadrupole magnets within the undulator section, can further improve the performance of x-ray vortices. Furthermore, Bayesian optimization is shown to be an effective and efficient strategy for optimizing undulator tapering, which will be beneficial for both design and online experiments of other FEL schemes in the future.

## ACKNOWLEDGEMENTS

We thank Serguei Molodtsov, Svitozar Serkez, and Christoph Lechner for useful discussions and for their interest in this work.

## REFERENCES

[1] L. Allen, M. W. Beijersbergen, R. Spreeuw, *et al.*, "Orbital angular momentum of light and the transformation of laguerre-gaussian laser modes," *Physical Review A* **45**(11), 8185 (1992).

[2] Y. Shen, X. Wang, Z. Xie, *et al.*, "Optical vortices 30 years on: Oam manipulation from topological charge to multiple singularities," *Light: Science & Applications* **8**(1), 1–29 (2019).

[3] M. van Veenendaal and I. McNulty, "Prediction of strong dichroism induced by x rays carrying orbital momentum," *Physical Review Letters* **98**(15), 157401 (2007).

[4] A. Picón, J. Mompart, J. V. de Aldana, *et al.*, "Photoionization with orbital angular momentum beams," *Optics Express* **18**(4), 3660–3671 (2010).

[5] A. S. Rury, "Examining resonant inelastic spontaneous scattering of classical laguerre-gauss beams from molecules," *Physical Review A* **87**(4), 043408 (2013).

[6] H. Yong, J. R. Rouxel, D. Keefer, *et al.*, "Direct monitoring of conical intersection passage via electronic coherences in twisted x-ray diffraction," *Physical Review Letters* **129**(10), 103001 (2022).

[7] N. Huang, H. Deng, B. Liu, *et al.*, "Features and futures of x-ray free-electron lasers," *The Innovation* **2**(2), 100097 (2021).

ISBN: 978-3-95450-231-8 ISSN: 2673-5490 doi: 10.18429/JACoW-IPAC2023-TUPL039



[8] G. Geloni, V. Kocharyan, and E. Saldin, "A Novel Self-Seeding Scheme for Hard X-Ray FELs," *Journal of Modern Optics* **58**(16), 1391–1403 (2011).

[9] C. Pellegrini, A. Marinelli, and S. Reiche, "The Physics of X-Ray Free-Electron Lasers," *Review of Modern Physics* **88**(1) (2016).

[10] A. G. Peele, P. J. McMahon, D. Paterson, *et al.*, "Observation of an x-ray vortex," *Optics Letters* **27**(20), 1752–1754 (2002).

[11] F. Seiboth, M. Kahnt, M. Lyubomirskiy, *et al.*, "Refractive hard x-ray vortex phase plates," *Optics Letters* **44**(18), 4622–4625 (2019).

[12] A. Sakdinawat and Y. Liu, "Soft-x-ray microscopy using spiral zone plates," *Optics Letters* **32**(18), 2635–2637 (2007).

[13] J. Vila-Comamala, A. Sakdinawat, and M. Guizar-Sicairos, "Characterization of x-ray phase vortices by ptychographic coherent diffractive imaging," *Optics Letters* **39**(18), 5281–5284 (2014).

[14] J. T. Lee, S. Alexander, S. Kevan, *et al.*, "Laguerre–gauss and hermite–gauss soft x-ray states generated using diffractive optics," *Nature Photonics* **13**(3), 205–209 (2019).

[15] P. R. Ribič, B. Rösner, D. Gauthier, *et al.*, "Extreme-ultraviolet vortices from a free-electron laser," *Physical Review X* **7**(3), 031036 (2017).

[16] E. Hemsing, "Coherent photons with angular momentum in a helical afterburner," *Physical Review Accelerators and Beams* **23**(2), 020703 (2020).

[17] E. Hemsing and A. Marinelli, "Echo-enabled x-ray vortex generation," *Physical Review Letters* **109**(22), 224801 (2012).

[18] P. R. Ribič, D. Gauthier, and G. De Ninno, "Generation of coherent extreme-ultraviolet radiation carrying orbital angular momentum," *Physical Review Letters* **112**(20), 203602 (2014).

[19] N. Huang and H. Deng, "Generating x-rays with orbital angular momentum in a free-electron laser oscillator," *Optica* **8**(7), 1020–1023 (2021).

[20] J. Yan and G. Geloni, "Self-seeded free-electron lasers with orbital angular momentum," *Adv. Photon. Nexus* **2**(3), 036001 (2023), https://doi.org/10.1117/1.APN.2.3.036001.

[21] J. Wu, X. Huang, T. Raubenheimer, A. Scheinker, and others, "Recent on-line taper optimization on LCLS," in *Proceedings, 38th International Free Electron Laser Conference, FEL*, 2018.

[22] J. Wu, N. Hu, H. Setiawan, X. Huang, T. O. Raubenheimer, Y. Jiao, G. Yu, A. Mandlekar, S. Spampinati, K. Fang, and others, "Multi-dimensional optimization of a terawatt seeded tapered free electron laser with a multi-objective genetic algorithm," *Nuclear Instruments and Methods in Physics Research Section A: Accelerators, Spectrometers, Detectors and Associated Equipment*, vol. 846, pp. 56–63, 2017.

[23] J. Močkus, "On Bayesian methods for seeking the extremum," in *Optimization Techniques IFIP Technical Conference: Novosibirsk, July 1–7, 1974*, pp. 400–404, Springer, 1975.

[24] B. Shahriari, K. Swersky, Z. Wang, R. P. Adams, and N. De Freitas, "Taking the human out of the loop: A review of Bayesian optimization," *Proceedings of the IEEE*, vol. 104, no. 1, pp. 148–175, 2015.

[25] M. Seeger, "Gaussian processes for machine learning," *International journal of neural systems*, vol. 14, no. 02, pp. 69–106, 2004.

[26] J. Wu, X.-Y. Chen, H. Zhang, L.-D. Xiong, H. Lei, and S.-H. Deng, "Hyperparameter optimization for machine learning models based on Bayesian optimization," *Journal of Electronic Science and Technology*, vol. 17, no. 1, pp. 26–40, 2019.

[27] J. Duris, D. Kennedy, A. Hanuka, J. Shtalenkova, A. Edelen, P. Baxevanis, A. Egger, T. Cope, M. McIntire, S. Ermon, and others, "Bayesian optimization of a free-electron laser," *Physical Review Letters*, vol. 124, no. 12, pp. 124801, 2020.

[28] R. J. Shalloo, S. J. D. Dann, J.-N. Gruse, C. I. D. Underwood, A. F. Antoine, C. Arran, M. Backhouse, C. D. Baird, M. D. Balcazar, N. Bourgeois, and others, "Automation and control of laser wakefield accelerators using Bayesian optimization," *Nature communications*, vol. 11, no. 1, pp. 6355, 2020.

[29] N. Srinivas, A. Krause, S. M. Kakade, and M. Seeger, "Gaussian process optimization in the bandit setting: No regret and experimental design," *arXiv preprint arXiv:0912.3995*, 2009.